Curved Electromagnetic Skins for Urban Scenarios

# Curved Electromagnetic Skins for Urban Scenarios

M. Beccaria[1], A. Freni[2], A. Mazzinghi[2], A. Massaccesi[1] P. Pirinoli[1]
[1]Dept. of Electronics and Telecommunications, Politecnico di Torino, Turin, Italy, paola.pirinoli@polito.it
[2]Department of Information Engineering, University of Florence, Florence, Italy; angelo.freni@unifi.it

***Abstract*—Recently, the possibility of increasing the performance of 5G and beyond wireless networks with the use of "smart electromagnetic skin" able to provide coverage in blind zones for a base station, is becoming an object of several studies. In this framework, the use of a curved configuration, which can be easily integrated into a cylindrical radome enclosing a street light or traffic light pole, is analyzed. The obtained numerical results prove that the proposed solution guarantees performance even better than a planar configuration occupying the same volume, with further advantages. In fact, it is simpler to mount, it has a lower visual impact, and it does not suffer from the influence of the supporting structure.**

***Index Terms*—Smart Electromagnetic Skin; Reflectarray; 5G antennas.**

## I. Introduction

In the next ten years, communication systems of the fifth generation and beyond will be asked to provide more functionality than those of the fourth generation. The analysis of the requirements they have to meet identifies the need for a higher transmission speed and very low latency as critical aspects. In fact, while there are not yet precise standards, the ambitious goals identified by next-generation wireless systems are the following: fast data transfer rates, corresponding to 1TB per second download speed; wide bandwidth availability; better coverage; almost zero latency (close to 0.1 msec); increase in overall data traffic and connected users; reduced energy consumption; capability of connecting intelligence rather than objects through the use of Artificial Intelligence (see for instance [1], [2], [3]). From preliminary studies, it comes to light that using mm-waves or sub-THz frequencies can be very promising since they would allow reaching an extremely high bandwidth, managing an ultra-high data rate, and providing quasi-negligible latency. On the other hand, these frequency bands suffer from higher free space loss, higher building penetration loss, and strong interaction with obstacles (e.g., foliage attenuation, rain attenuation, etc.) along the propagation path. Consequently, the coverage can be strongly degraded, if not completely absent, in regions not in the line of sight (LOS) of the base station antenna. The most straightforward solution for reducing these effects is increasing the number of base stations, but this would result in an undesired increase in the network complexity and, therefore, in its cost, its visual impact, and the electromagnetic pollution in the covered area. Recently, the definition of a Smart Electromagnetic Environment (SEE) in which the propagation environment is used to enhance the properties of the wireless system itself has been introduced as an efficient alternative. The basic idea is that of considering the environment no longer as a "passive" part of the wireless system, affecting the propagation in an uncontrollable way, but to design it in such a way that it actively contributes to improving the system performance (see, for example, [4], [5], [6]). The implementation of a SEE is possible thanks to the introduction of several active and passive devices that allow a significant improvement in the wireless network performance without increasing the number of base stations. Among them, Smart Electromagnetic Skins (SESs) [6]-[10] are very thin passive surfaces able to provide a not specular reflection to reach blind spots or cover desired areas. In addition, they must also satisfy constraints such as the reduced visual/environmental impact and the low cost. A more sophisticated version of SES is the so-called Reflecting Intelligent Surfaces (RISs) [11], [12], [13], able to provide some reconfigurability. In the following, the focus will be on entirely passive configurations. However, most of the discussed considerations are also valid for RIS.

Since they are assumed to be planar, a straightforward solution consists of integrating SESs into buildings' walls [6]-[10], so that their occupation and visual impact are reduced. However, this solution is not always feasible for the specific orientation of the building with respect to the base station, for buildings with plenty of windows, and for architectural heritage-restricted buildings in historical city centers. Thus, other supporting structures must be used. In this paper, the possibility of integrating a smart skin in a street light or a traffic light pole is investigated. The advantages of such a solution are several: the supporting structures belong to the urban furniture and, therefore, it is subject to fewer limitations; the SES can be rotated on the pole to maximize the link with the base station; the field re-radiated by the SES is not affected by the contribution of the wall, which could be not negligible [14]. In principle, a planar SES can also be adopted in this case. However, as will be discussed in the next Section, this is not the optimal solution, especially if the volume of the structure would be kept limited. The alternative presented here consists of using a curved SES, that can be easily located between the supporting pole and a concentric radome.

In the following, the main aspects of the curved SES design are discussed, and its comparison with a planar surface occupying the same volume is carried out; numerical results prove that the curved solution is feasible and that it guarantees even better performance than the planar one and that its features are slightly affected by the presence of a radome.

## II. Considered scenario

As a possible example, the scenario shown in Fig. 1a is considered. A base station is located on the border of a square (red dot in Fig. 1) at a height of 6.3 m and provides the 5G service in the millimeter band (26.5-27.5 GHz in Italy). It is assumed to consist of an $8 \times 8$ MIMO array that can cover a horizontal angular area of $\pm 60°$ [15].


(a)


(b)

Fig. 1. (a) Considered scenario. (b) Detail of a pole with the SES mounted on it and encapsulated in the radome.

In the square, several light poles (yellow dots in Fig. 1a) in the line of sight of the base station are already present. As schematically shown in Fig. 1a, if SESs are mounted on some of the poles, they provide the coverage of the streets adjacent to the square, that are not in the LOS of the base station, improving therefore the performance of the wireless network. The diameter of the poles depends on their height and it is not constant along it. In the following, the SES is supposed to be mounted at a height of 6.3 m in correspondence of which the pole diameter is assumed to be equal to 240 mm. To reduce the visual impact of the SES, it could be located between the pole and a cylindrical radome, with a diameter slightly larger than the pole one (here, it is taken equal to 300 mm), as shown in Fig. 1b.

## III. Curved SES design and analysis

As already highlighted, the aim of the present work is to assess the feasibility of a curved SES and to check if it is able to perform no worse than a planar surface occupying the same volume.

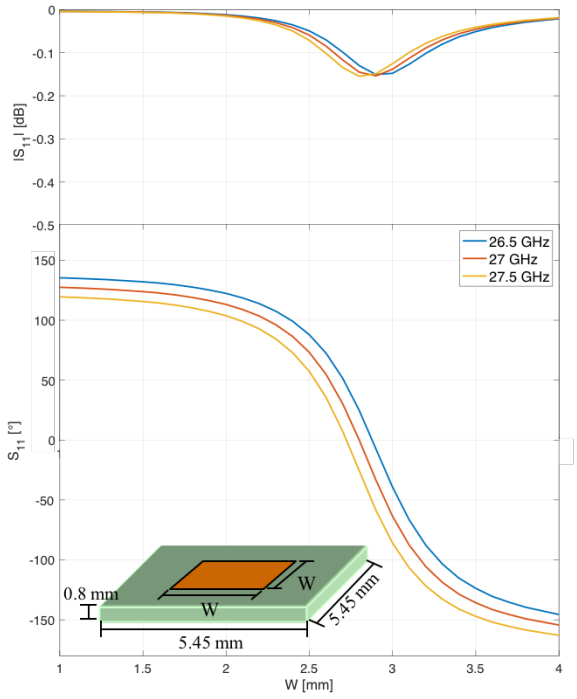


Fig. 2. Magnitude (top) and phase (bottom) of the reflection coefficient versus $W$ for different frequencies. Inset: unit cell geometry.

### A. Unit Cell

SESs can be designed using resonant unit cells, traditionally adopted for the realization of reflectarrays, or sub-wavelength ones, in which case they are conventionally referred to as metasurfaces. Here the first case is considered; the unit cell has a dimension of $5.45\,\text{mm} \times 5.45\,\text{mm}$ (i.e., $\lambda_0/2 \times \lambda_0/2$ at 27.5 GHz) and it is made of a square metallic patch of side $W$, as shown in the inset of Fig. 2, printed on a grounded dielectric DiClad527 substrate ($\varepsilon_r = 2.55$, $\tan\delta = 0.0022$), $h = 0.8\,\text{mm}$ thick. The choice of the substrate thickness is guided by the necessity to have a surface that can be curved, once the re-radiated elements are printed: as confirmed by the results in [16], the selected thickness allows the surface bending. The behavior of the unit cell is studied considering

that it is embedded in a periodic infinite lattice. This model can be used also for the case of the curved surface since the unit cell can be considered locally planar. The comparison among the phase curves as a function of $W$ obtained with an infinite periodic model, the analysis of a planar array of 5×5 elements, and a curved array with 5×5 elements, confirms that the utilized approximation provides sufficiently accurate results. In all the cases, the incident field is modeled with a plane wave, and different incident directions are considered.

Referring to the case of normal incidence, the variation of the amplitude (top) and phase (bottom) of $S_{11}$ with the size $W$ of the patch for three different frequencies inside the considered band is plotted in Fig. 2. Both the curves for the amplitude and phase computed at the different frequencies are very close to each other. $|S_{11}|$ is never lower than -0.2 dB, while the provided phase variation is almost 290° over the entire frequency range.

### *B. Comparison between curved and planar Smart Skins*

The unit cell described above is used for the design of two SESs, a curved one and a planar one, that can be both allocated between the pole and the radome. Both surfaces are designed considering the base station is sufficiently far that its radiated field when impinges on the SES is a plane wave. The direction of arrival of the incident wave is characterized by angles $\theta^i = 10°$ and $\phi^i = -90°$, while the re-radiated beam is assumed to point in $\theta^0 = 30°$, $\phi^0 = 70°$ with respect to the reference system shown in Figs. 3 and 4.

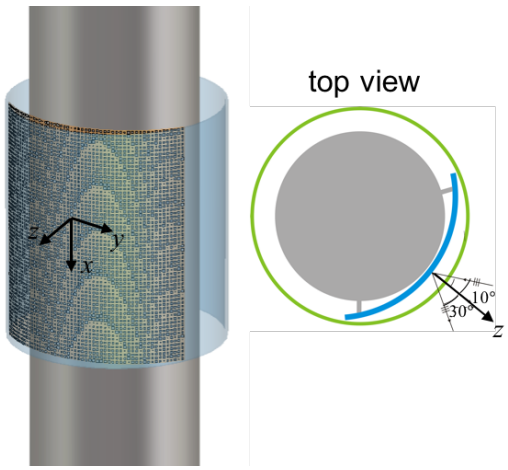


Fig. 3. 3D and top view of the curved smart skin located between the pole and the radome. The layout has been designed to obtain the pointing desired with the considered direction of arrival of the incident wave.

3D and top views of the considered geometry for the curved skin are shown in Figs. 3: the surface is not concentric to the pole and the radome, but has a radius of curvature of 175 mm, it is tangent to the pole in its central section and extend up to meet the radome. Its (curvilinear) width is therefore equal to 300 mm, while the chosen height is 340 mm. In view of the unit cell size, the SES layout consists therefore of $55 \times 62$ cells.

The geometry of the planar skin is instead depicted in Fig. 4. As the curved solution, also in this case, the SES is tangent to the pole in its central section and has a width of 180 mm that allows to locate it inside the cylindrical radome; in this way, the number of unit cells necessary to discretize the surface is $33 \times 62$. If a larger planar SES is used, it would be not possible to locate it between the pole and the radome, as it is in the considered case. A possible solution would be that of manufacturing an ad-hoc shaped radome, with the consequent increase in its volume and cost.

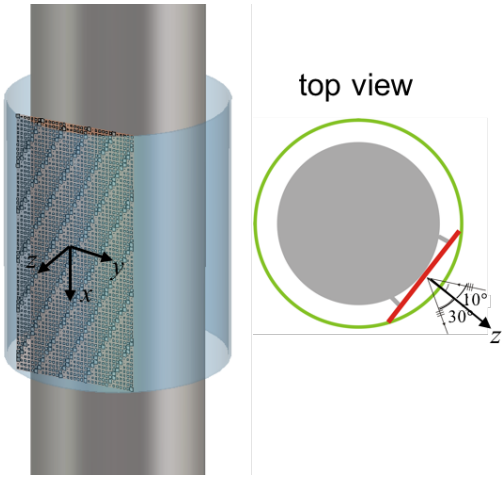


Fig. 4. 3D and top view of the planar smart skin located between the pole and the radome. The layout has been designed to obtain the desired pointing with the considered direction of arrival of the incident wave.

In Fig. 5 the Radar Cross Section [RCS] patterns in the vertical (top) and horizontal (bottom) planes with respect to the ground, at the three frequencies of 26.5, 27, and 27.5 GHz SES at 27.5 GHz are shown. The plots have been obtained through the full-wave simulation of the curved SES carried out with CST Microwave Studio [17]. It is worth noting that in the Figure, $\theta' = 0°$ corresponds to the nominal beam pointing direction $\theta^o = 30°$, $\phi^o = 70°$. The proper design enables compensating the effect introduced by the curvature, which would tend to spread the incident field: in the vertical plane, the RCSs evaluated at the three frequencies are almost overlapping, with side lobes lower than -15 dB; in the horizontal plane, the RCS is more asymmetrical and susceptible to frequency, with an increase of side lobes at 27.5 GHz. It can be partially ascribed to the choice of the unit cell, not optimized to have a wide band behavior.

Despite the increase of side lobes in the H plane, the variation of the maximum RCS within the considered band is lower than 1 dB, as it emerges from the plot in Fig. 6 (red line). In the same Figure also the frequency behavior of the maximum RCS for the planar skin is plotted (red line); the comparison between the results for the curved and planar SES confirms that the maximum value of the RCS obtained with the curved SES is never lower than that of the planar configuration, while at the central frequency, it is higher by approximately 3 dB and this means that the curved solution outperforms the

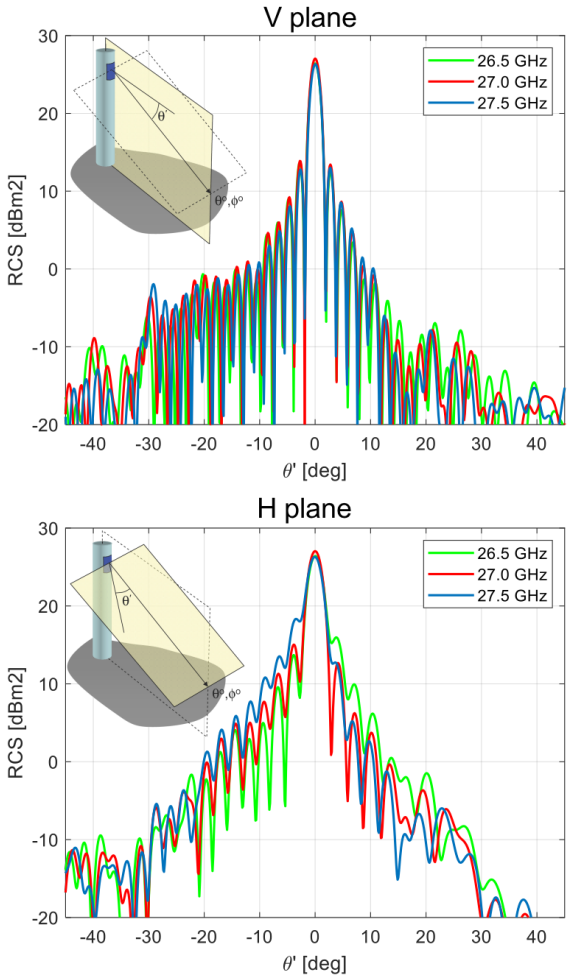


Fig. 5. RCS in the vertical (top) and horizontal (bottom) planes obtained through the simulation of the curved SES carried out with CST Microwave Studio at three different frequencies.

planar one, keeping the occupied volume equal.

In the same Figure, the frequency behavior of the maximum RCS for both the curved and planar SES evaluated taking into account the presence of the radome, is plotted. As already described in Sect. II, the internal radius of the radome is 150 mm. It is made of LEXAN$^{TM}$ ($\varepsilon_r = 2.8$, $\tan\delta = 0.01$) and has a thickness of 3.26 mm, corresponding to a quarter of the wavelength in the dielectric. The obtained RCS patterns, which are not shown for the sake of compactness, are very similar to those without the radome, but slightly lower. In fact, as appears comparing the curves in Fig. 6 related to the cases with or without the radome, the presence of this last is responsible for a decrease of the RCS, that at 27 GHz is of about 1.2 dB for both the curved and the planar skin.

### C. Example of real application

In view of the results summarized above, a curved SES has been designed to provide the link highlighted in magenta in Fig. 1a. The SES is located on a pole at a distance of 45 m from the base station, at its same height. Since the SES

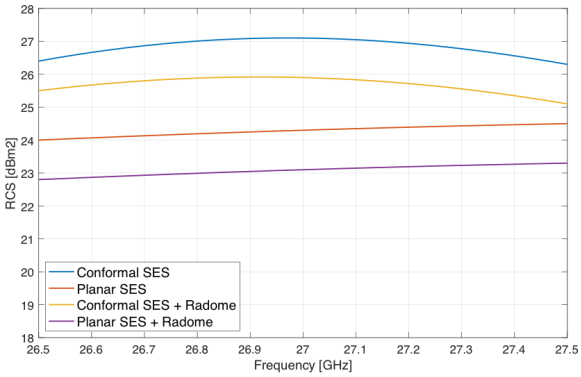


Fig. 6. Variation of maximum RCS with frequency: comparison between curved and planar SESs with and without the radome.

is in the far field region of the base station, and vice versa, the incident field can be modeled as a plane wave, whose direction of arrival forms an angle $\theta_i = 20°$ with the unit vector orthogonal to the SES surface on its center (i.e., the $z$-axis in Figure 3). To provide coverage to the street at its left, the SES has to focalize the incident field in a direction making 30° with respect to its $z$-axis.

A cosecant squared beam has to be generated in the vertical plane to illuminate the street surface uniformly. To this purpose, Powell's direction set algorithm (DSA) with implicitly constrained current elements [18] has been used to synthesize the phase of the scattered field on the SES aperture.

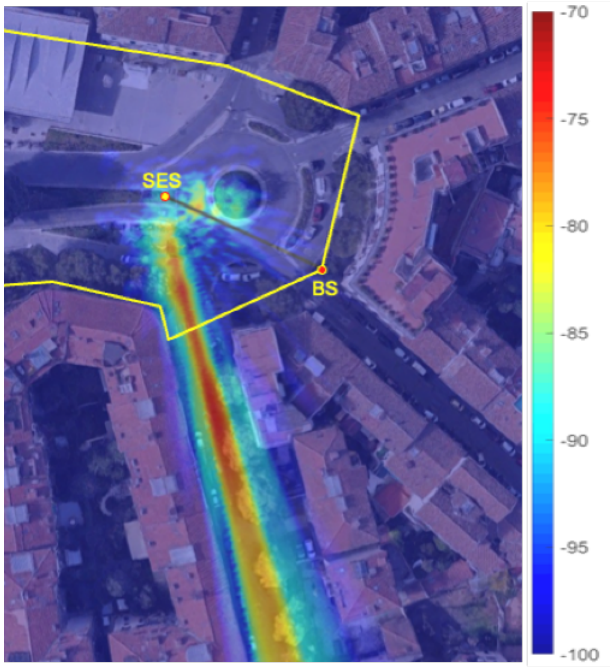


Fig. 7. Map of the simulated power density at ground level superimposed on the urban scenario.

The field scattered by the SES has been calculated by using CST Microwave Studio. Then, it field has been geo-referenced and calculated at ground level. Figure 7 shows the power density estimated at 27 GHz by also considering the path loss due to the distance of 45 m between the base station and the SES, and an EIRP of 30 dBm. As required, the coverage of the street has been obtained.

## IV. Conclusion

In the work, the possibility of integrating a smart electromagnetic skin with a light or traffic light pole to enhance the coverage of a base station operating in the 5G Italian millimeter band 26.5-27.5 GHz has been investigated. In particular, a solution based on the use of a curved surface has been considered: the comparison between a curved and a planar solution allocable under the same cylindrical radome, concentric to the pole, shows that the former solution performs better, with an increase of the RCS of more than 3 dB. The performance of the proposed solution has been finally analyzed in a real urban scenario: the results confirm that a curved SES can be profitably used in a millimeter wave 5G wireless system to enhance its capabilities.

## Acknowledgment

This research was carried out in the framework of the Italian National Recovery and Resilience Plan (NRRP) of NextGenerationEU, a partnership on "Telecommunications of the Future" (PE0000001 - program "RESTART").

## References

[1] H. Tataria, et al. "6G Wireless Systems: Vision, Requirements, Challenges, Insights, and Opportunities," Proc. of IEEE, vol. 109, pp. 1166–1199, 2021.

[2] M.Z. Chowdhury, M. Shahjalal, S. Ahmed and Y.M. Jang," 6G Wireless Communication Systems: Applications, Requirements, Technologies, Challenges, and Research Directions," IEEE Open Journal of the Communications Society, vol. 1, pp. 957–975, 2020.

[3] M. Matthaiou et al., "The Road to 6G: Ten Physical Layer Challenges for Communications Engineers," IEEE Communications Magazine, vol. 59, pp. 64–69, 2020.

[4] D. Erricolo, A. Rozhkova and A.C. Stutts, "Towards Smart Electromagnetic Environments," Proc. 2021 Computing, Communications, and IoT Applications (ComComAp), Shenzhen, China, 2021.

[5] R. Flamini et al., "Towards a Heterogeneous Smart Electromagnetic Environment for Millimeter-Wave Communications: An Industrial Viewpoint," IEEE Trans. Antennas Propag., vol. 70, pp. 8898–8910, 2022.

[6] G. Oliveri, et al., "Building a Smart EM Environment - AI-Enhanced Aperiodic Micro-Scale Design of Passive EM Skins," IEEE Trans. Antennas Propag., vol. 70, pp. 8757–8770, 2022.

[7] G. Oliveri, P. Rocca, M. Salucci and A. Massa, "Holographic Smart EM Skins for Advanced Beam Power Shaping in Next Generation Wireless Environments," IEEE Jou. Multiscale and Multiph. Comp. Tech., vol. 6, pp. 171–182, 2021.

[8] P. Rocca et al., "On the Design of Modular Reflecting EM Skins for Enhanced Urban Wireless Coverage," IEEE Trans. Antennas Propag., vol. 70, pp. 8771–8784, 2022.

[9] G. Oliveri et al., "Constrained Design of Passive Static EM Skins," IEEE Trans. Antennas Propag., vol. 71, pp. 1528–1538, 2023.

[10] E. Martinez-de-Rioja et al., "Passive intelligent reflecting surfaces based on reflectarray panels to enhance 5G millimeter-wave coverage," Int. Journal of Microw. and Wireless Tech., vol. 15, pp. 1–12, 2022.

[11] E. Basar, et al., "Wireless Communications Through Reconfigurable Intelligent Surfaces," IEEE Access, vol. 7, pp. 116753–116773, 2019.

[12] M. Di Renzo et al., "Smart Radio Environments Empowered by Reconfigurable Intelligent Surfaces: How It Works, State of Research, and The Road Ahead," IEEE Journal on Selected Areas in Comm., vol. 38, pp. 2450–2525, 2022.

[13] Q. Wu, et al., "Intelligent Reflecting Surface-Aided Wireless Communications: A Tutorial," IEEE Trans. Commun., vol. 69, pp. 3313–3351, 2021.

[14] A.F. Vaquero, E. Martinez-de-Rioja, M. Arrebola, and J.A. Encinar, "Study on the Effect of the Wall in the Performance of an Intelligent Reflective Surface for Providing Coverage in mm-Wave Frequencies," Proce. European Conf. on Antennas and Propag. (EuCAP), Florence, Italy, 2023.

[15] Future Access 28Ghz Phased Array Antenna Module (PAAM), 2023 [Online] https://mmwavetech.fujikura.jp/5g/

[16] M. Beccaria, P. Pirinoli, G. Dassano, and M. Orefice, "Design and experimental validation of convex conformal reflectarray antennas," Electron. Lett., vol. 52 pp. 1511-1512, 2016.

[17] CST Microwave Studio, 2023 [online]. Available: http://www.cst.com/

[18] M.J. Buckley, "Synthesis of Shaped Beam Antenna Pattern Using Implicit Constrained Current Elements," IEEE Trans. Antennas Propag., vol. 44, pp. 192–197, 1996.